Analysis of Spectral Data

Jayson Purl

April 23, 2025

1 Introduction

This report presents the results of a spectral analysis conducted on a set of survey objects. The primary goals of this analysis were to classify the spectra of the objects, determine their redshift values, and estimate their distances. Additionally, we aimed to describe key spectral features that provide insights into the physical properties and activity of the objects.

Spectral classification allows us to categorize objects, such as galaxies, quasars, and stars, based on their unique spectral signatures. The redshift values were derived from the observed shifts in spectral lines, providing an estimate of the objects' velocities and enabling us to calculate their distances using Hubble's Law.

By analyzing specific spectral features, such as emission and absorption lines, we could investigate the presence of active processes, such as star formation or accretion, and identify important characteristics of the objects, including their gas composition and physical conditions. This analysis is critical for understanding the universe's distribution and evolution of these objects.

2 Data Analysis

The program analyzes the spectral data of objects from a 10 arcmin cone in the sky centered at 3C 273. The data is obtained from SDSS. SDSS spectra undergo SDSS's data pipelines, which helps scientists analyze their data more efficiently. This pipeline does a preliminary classification of the target object, finds its redshift, and compiles a list of all important spectral features that may be present. All of this data is stored with the spectrum in a FITS file.

2.1 Wavelength Calibration

First, the program extracts the wavelength and flux data from the FITS file. The redshift is also extracted from the FITS file to perform wavelength calibration. The wavelength values are converted from the observed frame to the rest frame by dividing them by $1 + z$, where z is the redshift.

$$\lambda_{\text{rest}} = \frac{\lambda_{\text{observed}}}{1 + z}$$

This ensures that the spectral features align with their rest-frame positions, accounting for the universe's expansion.

2.2 Distance and Recession Velocity

The program calculates the recession velocity of the object using the formula:

$$v_{\text{radial}} = z \times c$$

where z is the redshift and $c = 299,792.458\,\text{km/s}$ is the speed of light. The distance to the galaxy is then computed using Hubble's law:

$$d = \frac{v_{\text{radial}}}{H_0}$$

where $H_0 = 70\,\text{km/s/Mpc}$ is the Hubble constant. The resulting distance is given in megaparsecs (Mpc).

2.3 Spectral Line Analysis

The program extracts spectral lines from the SPZLINE extension of the FITS file. For each spectral line, the program calculates the Full Width at Half Maximum (FWHM) from the LINESIGMA (σ) value:

$$FWHM = 2 \times \sigma$$

the velocity width using the following equation:

$$v_{\text{width}} = \frac{\text{FWHM}}{\lambda_{\text{rest}}} \times c$$

and the equivalent width (EW) using trapezoidal integration:

$$EW = \int \left(1 - \frac{F_\lambda}{F_{\text{cont}}}\right) \Delta\lambda$$

where F_λ is the flux at wavelength λ and F_{cont} is the continuum flux near the line.

2.4 Galaxy Classification

The FITS files contain data on the object's class. Objects are classified as STAR, GALAXY, or QSO. The class is determined from this label, but for subtypes of the galaxies, the spectra are plotted to determine if there is a larger red population or blue population of stars and to determine if there is large star formation. Along with optical imaging, the galaxies can be classified as spiral, elliptical, or starbursts.

3 Results

The analysis of the survey objects revealed distinct spectral characteristics across the different types of objects. Quasars were found to have high redshifts, with spectra that differed significantly from those of galaxies and stars. Their spectra prominently featured Ly-alpha, N V, and C IV emission lines, with large Full Width at Half Maximum (FWHM) values, indicating the presence of highly energetic processes in these objects.

For the galaxies, the spectra mostly showed [O II] and [Ne III] emission lines, typical of star-forming galaxies. The objects displayed a wide range of distances, as seen in the Hubble Diagram, where more distant objects showed larger recessional velocities following Hubble's Law.

The spectra of the spiral/starburst galaxies displayed a bluer continuum, indicative of ongoing star formation and large emission lines associated with active H II regions. In contrast, elliptical galaxies exhibited a redder continuum with a characteristic low flux below 4500 Å, marking the presence of older stellar populations. Elliptical galaxies also displayed a notable broad Ar III absorption feature, distinguishing them from other galaxy types.

Overall, the spectral analysis highlighted clear differences in the objects' physical conditions and evolutionary stages, with star formation marked by strong emission lines and older stellar populations in elliptical galaxies marked by absorption features and a redder continuum. The table at the back of the appendix shows each spectrum's important characteristics.

4 Appendix

4.1 Figure 1

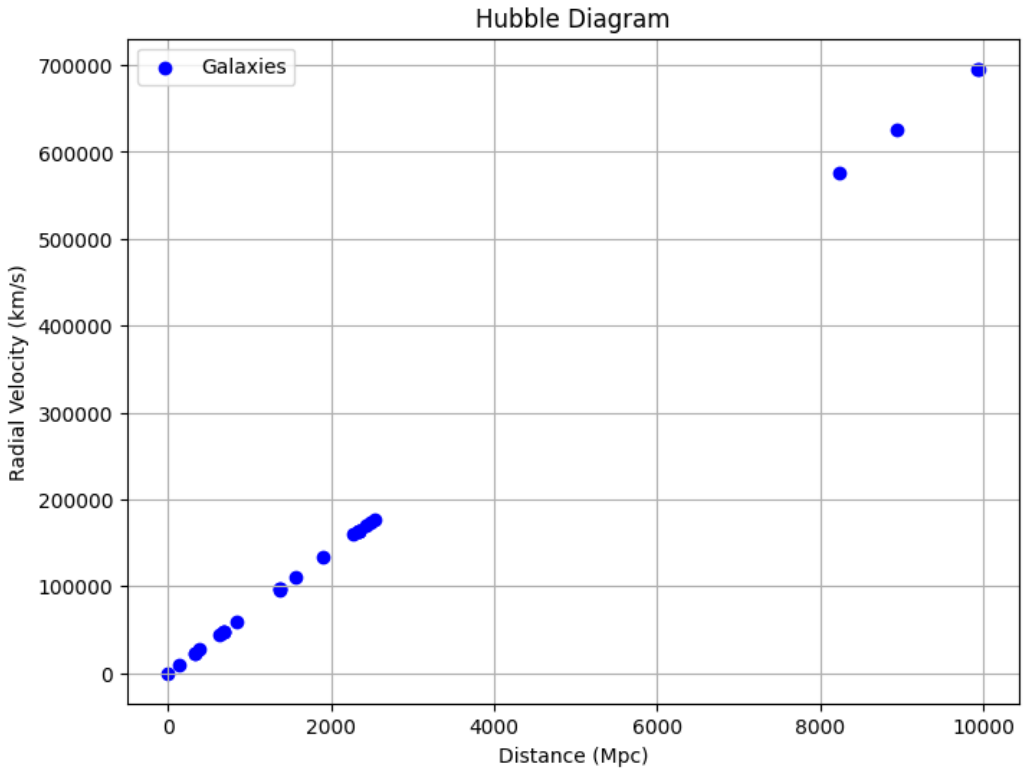

Figure 1: Hubble Diagram showing the relationship between recession velocity and distance for the galaxies in the sample.

4.2 Figure 2

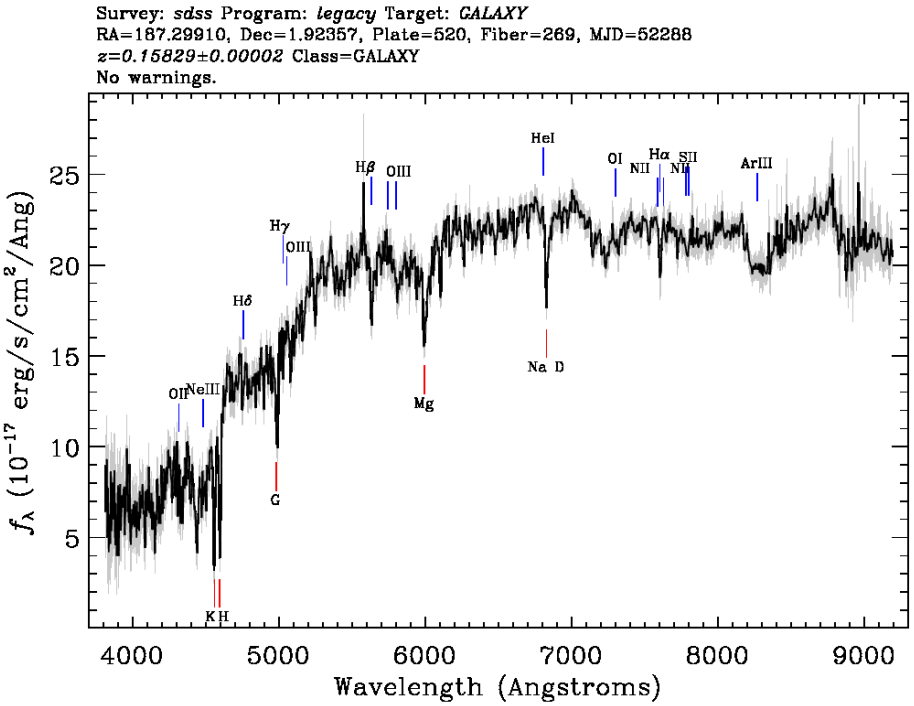

Figure 2: Spectral plot of an elliptical galaxy

4.3 Figure 3

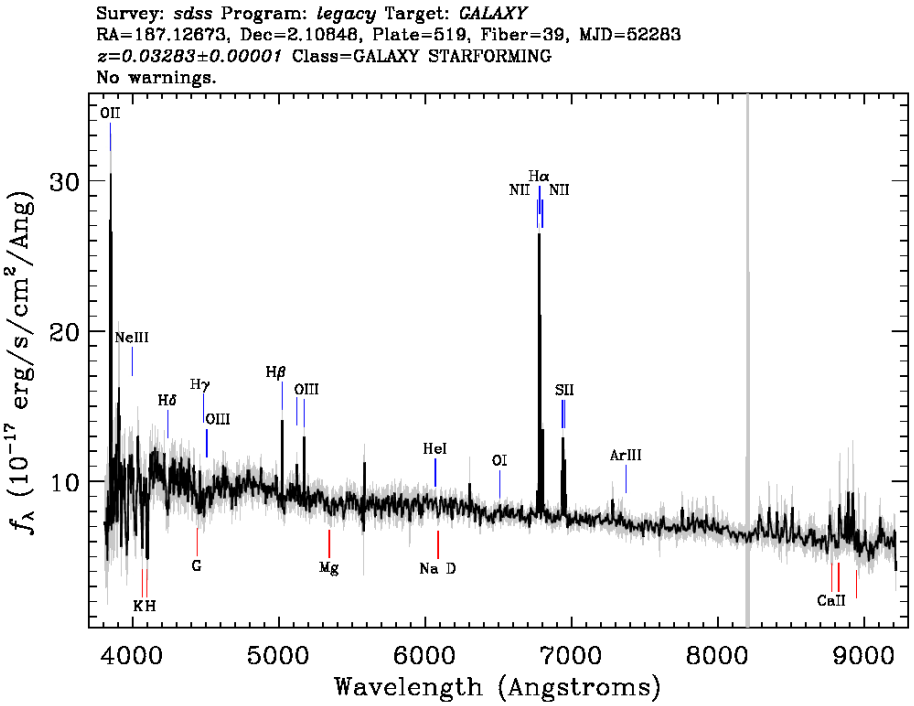

Figure 3: Spectral plot of a spiral galaxy

4.4 Figure 4

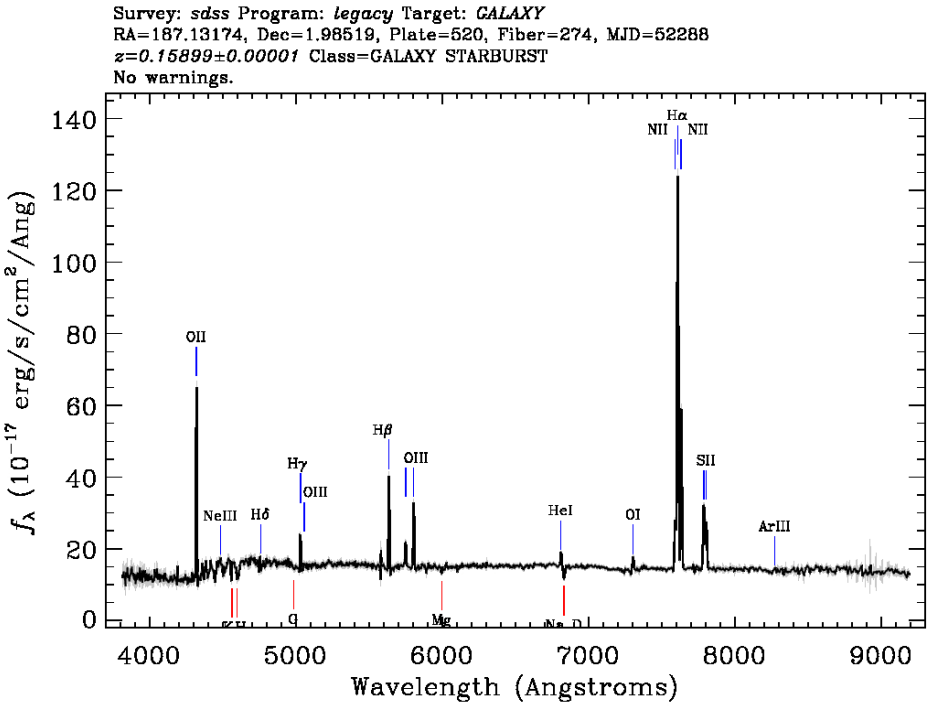

Figure 4: Spectral plot of a starburst galaxy

4.5 Figure 5

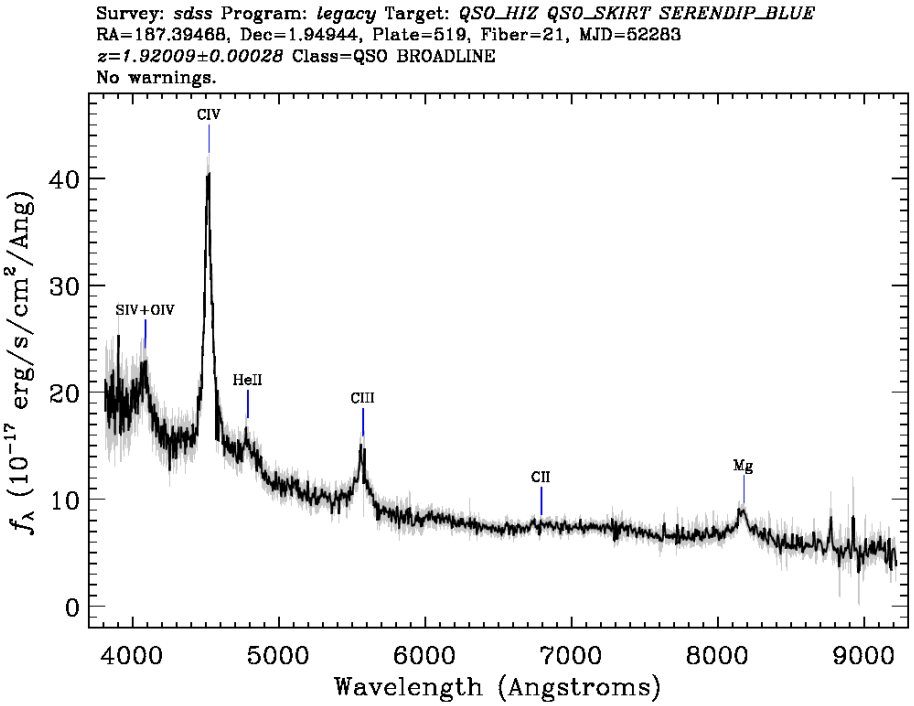

Figure 5: Spectral plot of a QSO AKA quasar

4.6 Table 1

Spectrum Name	Object Type	Subtype	Redshift	Distance (Mpc)	Recession Velocity (km/s)
spec-4752-55653-0217	GALAXY	ELLIPTICAL	0.5786812	2478.3464	173484.25
spec-4752-55653-0277	GALAXY	ELLIPTICAL	0.5458756	2337.8484	163649.39
spec-0520-52288-0270	GALAXY	ELLIPTICAL	0.15886477	680.378	47626.46
spec-0519-52283-0023	GALAXY	ELLIPTICAL	0.07779926	333.19476	23323.633
spec-0519-52283-0039	GALAXY	SPIRAL STARFORMIN	0.032827772	140.59312	9841.519
spec-0519-52283-0028	GALAXY	SPIRAL STARFORMIN	0.14656785	627.7134	43939.938
spec-4752-55653-0211	GALAXY	ELLIPTICAL	0.5686625	2435.439	170480.73
spec-4752-55653-0210	GALAXY	ELLIPTICAL	0.5478763	2346.417	164249.19
spec-0519-52283-0029	GALAXY	ELLIPTICAL	0.07727579	330.95285	23166.7
spec-4752-55653-0272	GALAXY	ELLIPTICAL	0.36735785	1573.3016	110131.12
spec-4752-55653-0264	QSO		2.3162024	9919.715	694380.06
spec-0519-52283-0030	GALAXY	ELLIPTICAL	0.09001823	385.52554	26986.787
spec-4752-55653-0268	GALAXY	ELLIPTICAL	0.31989294	1370.0214	95901.49
spec-4752-55653-0213	GALAXY	ELLIPTICAL	0.5456068	2336.6973	163568.81
spec-0520-52288-0280	STAR	K7	-0.00019338554	-0.82822186	-57.97553
spec-4752-55653-0212	GALAXY	ELLIPTICAL	0.3216214	1377.4238	96419.67
spec-0520-52288-0278	GALAXY	ELLIPTICAL	0.5470484	2342.871	164000.98
spec-0520-52288-0274	GALAXY	STARBURST	0.15898918	680.9108	47663.758
spec-4752-55653-0215	GALAXY	STARBURST	0.19736384	845.2599	59168.19
spec-0520-52288-0269	GALAXY	ELLIPTICAL	0.15829028	677.91766	47454.234
spec-4752-55653-0274	GALAXY	ELLIPTICAL	0.5906017	2529.3992	177057.94
spec-4752-55653-0262	QSO		2.3200119	9936.029	695522.06
spec-4752-55653-0219	GALAXY	ELLIPTICAL	0.44434887	1903.0348	133212.44
spec-0520-52288-0264	GALAXY	ELLIPTICAL	0.32181787	1378.2654	96478.58
spec-4752-55653-0218	QSO		2.0855567	8931.917	625234.2
spec-0519-52283-0021	QSO		1.9200873	8223.254	575627.75
spec-4752-55653-0280	GALAXY	ELLIPTICAL	0.5323155	2279.774	159584.17

Spectrum Name	Largest Features	FWHM (Å)	Velocity Width (km/s)	Equivalent Width (km/s)
spec-4752-55653-0217	Mg_II 2799, [O_II] 3725, [O_II] 3727	622.72, 622.72, 622.72	66665.92, 50088.81, 50051.42	12.27,1.83,2.33
spec-4752-55653-0277	H_zeta, Mg_II 2799, H_epsilon	277.33, 197.88, 277.33	21372.46, 21184.48, 20936.36	4.05,12.27,5.24
spec-0520-52288-0270	[O_II] 3725 , [O_II] 3727 , [Ne_III] 3868	698.66, 698.66, 698.66	56197.40, 56155.46, 54124.19	1.83,2.33,2.71
spec-0519-52283-0023	[O_II] 3725 , [O_II] 3727 , [Ne_III] 3868	816.52, 816.52, 816.52	65677.47, 65628.45, 63254.53	1.83,2.33,2.71
spec-0519-52283-0039	[O_II] 3725 , [O_II] 3727 , H_epsilon	168.28, 168.28, 171.40	13535.97, 13525.87, 13208.56	1.83,2.33,4.05
spec-0519-52283-0028	[O_II] 3725 , [O_II] 3727 , [Ne_III] 3868	285.21, 285.21, 285.21	22941.46, 22924.34, 22095.12	1.83,2.33,2.71
spec-4752-55653-0211	Mg_II 2799, [O_II] 3725, [O_II] 3727	1103.56, 1103.56, 1103.56	118143.70, 88766.16, 88699.91	12.27,1.83,2.33
spec-4752-55653-0210	Mg_II 2799, [O_II] 3725, [O_II] 3727	721.05, 721.05, 721.05	77193.39, 57998.53, 57955.24	12.27,1.83,2.33
spec-0519-52283-0029	[O_II] 3725 , [O_II] 3727 , [Ne_III] 3868	647.84, 647.84, 647.84	52109.55, 52070.66, 50187.15	1.83,2.33,2.71
spec-4752-55653-0272	Mg_II 2799, [O_II] 3725, [O_II] 3727	2546.12, 2546.12, 2546.12	272579.67, 204800.16, 204647.32	12.27,1.83,2.33
spec-4752-55653-0264	Ly_alpha, N_V 1240, C_IV 1549	7872.61, 3787.91, 3047.17	1941437.96, 915198.11, 589564.22	0.00,0.00,0.00
spec-0519-52283-0030	[O_II] 3725 , [O_II] 3727 , [Ne_III] 3868	766.43, 766.43, 766.43	61648.88, 61602.87, 59374.56	1.83,2.33,2.71
spec-4752-55653-0268	Mg_II 2799, [O_II] 3725, [O_II] 3727	996.61, 996.61, 996.61	106694.17, 80163.66, 80103.83	12.27,1.83,2.33
spec-4752-55653-0213	Mg_II 2799, H_zeta, H_epsilon	578.72, 736.61, 736.61	61956.37, 56766.23, 55607.91	12.27,4.05,5.24
spec-0520-52288-0280	H_epsilon , H_delta , H_beta	1037.69, 1037.69, 1037.69	79968.81, 75822.31, 63975.12	4.05,-0.48,-5.39
spec-4752-55653-0212	Mg_II 2799, H_zeta, H_epsilon	582.07, 734.73, 734.73	62314.65, 56621.18, 55465.82	12.27,4.05,5.24
spec-0520-52288-0278	Mg_II 2799 , [O_II] 3725 , [O_II] 3727	268.64, 268.64, 268.64	28759.33, 21608.05, 21591.92	12.27,1.83,2.33
spec-0520-52288-0274	[O_II] 3725 , [O_II] 3727 , [Ne_III] 3868	380.17, 380.17, 380.17	30579.27, 30556.44, 29451.15	1.83,2.33,2.71
spec-4752-55653-0215	[O_II] 3725, [O_II] 3727, [Ne_III] 3868	305.01, 305.01, 305.01	24533.82, 24515.51, 23628.73	1.83,2.33,2.71
spec-0520-52288-0269	[O_II] 3725 , [O_II] 3727 , [Ne_III] 3868	902.60, 902.60, 902.60	72601.27, 72547.08, 69922.89	1.83,2.33,2.71
spec-4752-55653-0274	H_zeta, H_epsilon, H_delta	797.21, 797.21, 797.21	61436.12, 60182.52, 58250.80	4.05,5.24,-0.48
spec-4752-55653-0262	N_V 1240, Ly_alpha, C_IV 1549	7334.97, 3933.39, 4899.43	1772205.19, 970001.26, 947938.80	0.00,0.00,0.00
spec-4752-55653-0219	Mg_II 2799, [O_II] 3725, [O_II] 3727	590.57, 590.57, 590.57	63224.27, 47502.96, 47467.51	12.27,1.83,2.33
spec-0520-52288-0264	[O_II] 3725 , [O_II] 3727 , [Ne_III] 3868	1155.19, 1155.19, 1155.19	92918.83, 92849.48, 89490.91	1.83,2.33,2.71
spec-4752-55653-0218	N_V 1240, Ly_alpha, C_IV 1549	21140.14, 6472.03, 7737.11	5107674.46, 1596047.24, 1496971.27	0.00,0.00,0.00
spec-0519-52283-0021	C_IV 1549 , He_II 1640 , C_III] 1908	4246.39, 4246.39, 4246.39	821588.91, 776042.47, 666952.85	0.00,0.00,0.00
spec-4752-55653-0280	H_zeta, H_epsilon, H_delta	453.21, 453.21, 453.21	34926.50, 34213.82, 33115.64	4.05,5.24,-0.48